Structure and Interactions in Large Compound Particles Formed by Polyglycidol-Based Analogues to Pluronic Copolymers in Aqueous Solution

S. Halacheva,[†] S. Rangelov,*[,†] and V. M. Garamus[‡]

Institute of Polymers, Bulgarian Academy of Sciences, Acad. G. Bonchev 103-A, 1113 Sofia, Bulgaria, and GKSS Research Centre, Max-Planck Strasse 1, D-21502 Geesthacht, Germany

Received May 22, 2007; Revised Manuscript Received August 8, 2007

ABSTRACT: Large compound particles formed in water by polyglycidol−poly(propylene oxide)−polyglycidol, PG−PPO−PG, block copolymers are investigated by small-angle neutron scattering. The present PG-based copolymers differ from the familiar Pluronic copolymers in that the poly(ethylene oxide) blocks of the latter are substituted by structurally similar blocks of PG bearing a hydroxyl group in each monomer unit. The temperature and concentration intervals covered in this study were 15−60 °C and 2−33 wt %, respectively. The results reveal that in the interior of the large particles slightly prolate spherical PPO domains coexist with individual chains. The latter are not involved in the formation of the PPO domains but mediate interdomain interactions via hydrogen bonding. The dimensions of the two types of scattering objects as well as the aggregation number of the PPO domains were determined. The number of the PPO domains per large compound particle was estimated at different temperatures using earlier light scattering data. At higher concentrations the PPO domains are arranged in a cubic lattice. Their surface is sharper and more distinct at 60 °C than at 40 °C.

Introduction

Poly(ethylene oxide)−poly(propylene oxide)−poly(ethylene oxide) (PEO−PPO−PEO) block copolymers (commonly known under the trade name Pluronic) are polymeric nonionic surfactants that are commercially available in wide ranges of molecular weights and ratios of the constituent blocks. Their self-assembly in aqueous solution has attracted the interest of both academia and industry. It is generally accepted that above a certain critical concentration and temperature, referred to as critical micellization concentration (cmc) and critical micellization temperature (cmt), respectively, the copolymers self-associate into aggregates. These are typically described as spherical objects with a core consisting of mainly PPO and a corona of hydrated swollen PEO chains interacting with water. Upon a further increase of temperature and/or concentration often a transition from spherical to another, e.g., rodlike, morphology takes place, and a variety of ordered phases has been documented.[1−17] Practically all known liquid-crystalline phases, such as cubic, hexagonal, lamellar, and bicontinuous, as well as reverse phases have been reported.[9−17] The proven commercial utility of the Pluronic copolymers has led to further research to find novel copolymer architectures and compositions that would broaden the surfactant properties and characteristics. As a result, PEO−PPO as well as PEO−PBO (here, PBO denotes poly(butylene oxide)) copolymers of diblock, reverse triblock, and starlike chain architectures have been commercialized or prepared in laboratory scales and quantities and extensively investigated.[18−22] To the best of our knowledge, no attempts have been made to replace PEO with other hydrophilic chains. In recent studies the synthesis and aqueous solution properties of a series of analogues to Pluronic copolymers have been described.[23,24] In these copolymers the flanking blocks of PEO were substituted by blocks of its structural analogue polyglycidol, PG. PG, in contrast to PEO, bears a hydroxyl group in each monomer unit. Figure 1 shows the structural formulas of the monomer units of PEO, PPO, and PG. The copolymers of the series described elsewhere[23,24] have a middle block of PPO with a common degree of polymerization of 34 and ranging from 3 to 70 degrees of polymerization of the flanking PG blocks, thus making them closest in composition to Pluronic series L61−F68 and L72−F77. The aqueous solution properties of the novel copolymers[23] are in some aspects similar to those of the corresponding Pluronic copolymers; for example, the cmcs increase with increasing hydrophilic component content or decreasing temperature. There are, however, a number of aspects in which the PG-based copolymers (hereinafter LGP copolymers) differ from their Pluronic analogues. Although still entropy-driven, the process of self-association of the LGP copolymers is somewhat entropically less favored with a lower enthalpic barrier to aggregation compared to that of the Pluronic copolymers.[23] The most striking, however, are the differences in the hydrodynamic dimensions and aggregation numbers of the particles, which are considerably larger than those of the familiar Pluronic micelles.[24] On the basis of the results from light scattering and cryogenic transmission electron microscopy, a plausible model of the particle structure has been proposed.[24] According to this model, the LGP nanoparticles provide a coherent interior consisting of discontinuous, compact, hydrophobic domains built of PPO, which are dispersed in a considerably less compact medium of PG and water. Two attractive processes are equally involved

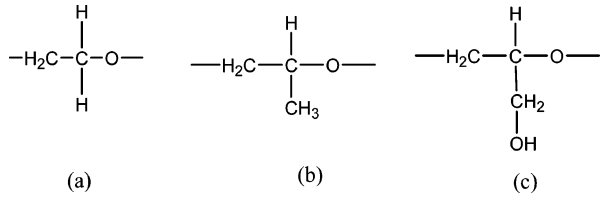

Figure 1. Monomer units of (a) poly(ethylene oxide), (b) poly(propylene oxide), and (c) linear polyglycidol.

* Corresponding author: Tel + 359 2 9792293, Fax + 359 2 8700309, e-mail rangelov@polymer.bas.bg.
[†] Bulgarian Academy of Sciences.
[‡] GKSS Research Centre.

10.1021/ma071151q CCC: $37.00
Published on Web 10/03/2007

Table 1. Abbreviations, Composition, Polyglycidol Content, and Total Molecular Weight of the Copolymers Used in This Study[a]

abbreviation	composition	PG content (wt %)	mol wt[b]
LGP63	$(G)_6(PO)_{34}(G)_6$	30	2900
LGP67	$(G)_{26}(PO)_{34}(G)_{26}$	70	5800
LGP68	$(G)_{51}(PO)_{34}(G)_{51}$	80	9500
LGP68+	$(G)_{70}(PO)_{34}(G)_{70}$	84	12400

[a] G and PO denote polyglycidol and poly(propylene oxide) monomer units, respectively. [b] Calculated from ^{1}H NMR data (see ref 23).

in the particle formation: hydrophobic interactions of the PPO blocks and formation of multiple intra- and interchain hydrogen bonds involving the hydroxyl groups of the PG moieties.

Motivated by these results, the aim of the present work was to further extend the study by quantifying the size of the PPO domains inside the large compound particles and following possible structural changes and disorder to order transitions with temperature, concentration, and PG content. Small-angle neutron scattering (SANS) was used as a main technique. SANS has made a major impact on the understanding of polymer conformations, morphology, rheology, and thermodynamics.[25] It is a well-established method for characterizing the microstructure of various materials including micellar systems[12a,26] and, more specifically, Pluronic copolymers and their aqueous and nonaqueous solutions.[12a,14b,16,27] For the present study we have selected four PG−PPO−PG copolymers of a common degree of polymerization of the middle block of PPO of 34 and varying from 6 to 70 degrees of polymerization of the flanking PG blocks. In Table 1, the abbreviations, compositions, PG contents, and molecular weights of the selected copolymers are presented. The measurements were carried out in extended concentration (from 2 to 33 wt %) and temperature (15−60 °C) ranges.

Experimental Section

Materials and Sample Preparation. The copolymers used in the present study were synthesized as described elsewhere.[23] They are symmetric triblock copolymers of a general formula $(G)_n(PO)_{34}(G)_n$, where G and PO denote glycidol and propylene oxide, respectively, and n varies from 6 to 70, corresponding to PG content from 30 to 84 wt %. The composition, PG content, total copolymer molecular weight, and the codes of the copolymers are given in Table 1. Solutions in D_2O in the concentration range from 2 to 33 wt % were prepared by dilution of stock solutions. The latter were prepared gravimetrically by adding D_2O to preweighted quantity of the copolymer and allowed to mix overnight by shaking occasionally. The additional amount of D_2O was added to get solutions of desired concentrations. D_2O with D purity higher than 99.8% was a product of Aldrich.

Small-Angle Neutron Scattering. The SANS experiments were performed at the SANS1 instrument at the FRG1 research reactor at GKSS Research Centre, Geesthacht, Germany.[28] The range of scattering vectors q from 0.005 to 0.26 Å^{-1} was covered by four sample-to-detector distances (from 0.7 to 9.7 m). The neutron wavelength was 8.1 Å, and the wavelength spread of the mechanical velocity selector was 10% (fwhm). The samples were kept in quartz cells (Helma, Germany) with a path length of 2 or 5 mm, depending on copolymer concentration. The sample transmissions were invariably higher than 70%, indicating that the effects of multiple scattering are negligible. For isothermal conditions, a thermostated sample holder was used. The raw spectra were corrected for backgrounds from the solvent, sample cell, and other sources by conventional procedures. The two-dimensional isotropic scattering spectra were azimuthally averaged, converted to absolute scale, and corrected for detector efficiency by dividing by the incoherent scattering spectrum of pure water, which was measured with a 1 mm path length quartz cell. The smearing induced by the different instrumental settings was included in the data analysis.[29]

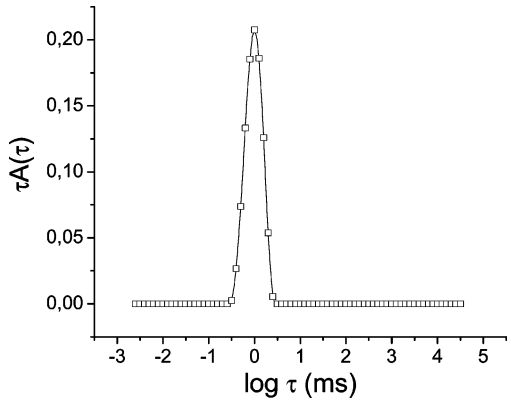

Figure 2. An example of relaxation time distribution from dynamic light scattering measured at an angle of 90° for an aqueous dispersion of LGP68 at 15.4 mg mL^{-1} and 40 °C.

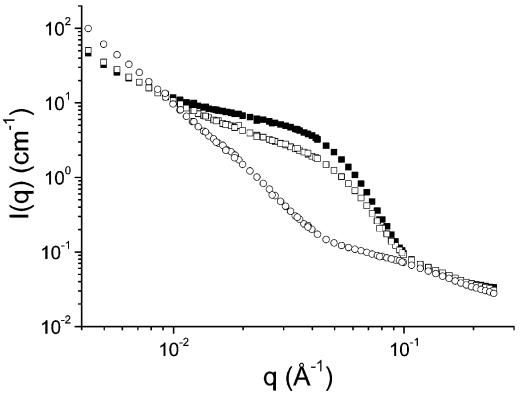

Figure 3. SANS data for a 2.12 wt % aqueous solution of LGP67 at 15 (open circles), 40 (open squares), and 60 °C (closed squares).

Results and Discussion

General Remarks. The four copolymers selected for the present study (Table 1) self-associate in water above a cmc and in dilute limit show a monomodal distribution from dynamic light scattering, which is preserved in the investigated concentration and temperature ranges.[24] An example of a relaxation time distribution function for LGP68 at 40 °C is presented in Figure 2. The particle sizes and aggregation numbers, which for the present selection of copolymers are in the ranges ca. 60−160 nm and 140−2080 macromolecules per particle, respectively, were found to decrease with increase of both PG content and temperature.[24]

The samples for SANS were prepared as solutions in D_2O at concentrations covering the range from 2 to 33 wt %. They looked transparent to moderately opalescent at room temperature. Phase separation was observed for some of the solutions of LGP63 at elevated temperatures. Therefore, the results for this copolymer are only occasionally presented.

Low Concentrated Solutions. General Features of Scattering Patterns. The SANS data obtained in this concentration region are presented in Figures 3 and 4. In particular, Figure 3 shows the scattering profiles obtained for the 2.12 wt % solution of LGP67 at 15, 40, and 60 °C, whereas Figure 4 presents the effect of the copolymer composition on the shape of the scattering profiles at different temperatures. The scattering data were first analyzed by slope determination, i.e., $I(q) \sim q^{-\alpha}$. The slopes at different q ranges were calculated and presented in Table 2. At the lowest q range traces of scattering from very large (>100 nm) particles are seen, which is in good agreement to the light scattering data.[24] The latter showed that the size of the particles are dependent on temperature. Therefore, the

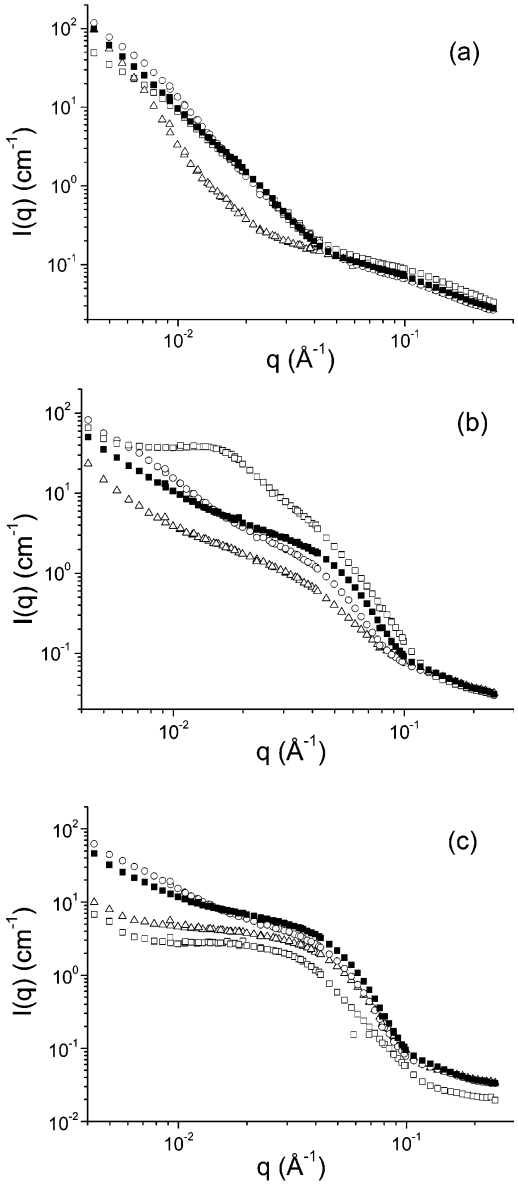

Figure 4. Effect of the copolymer composition on the shape of the scattering profiles at (a) 15, (b) 40, and (c) 60 °C. Symbols and concentrations: 2.15 wt % of LGP63 (open squares), 2.12 wt % of LGP67 (closed squares), 2.15 wt % of LGP68 (open circles), and 2.15 wt % of LGP68+ (open triangles).

crossings of the scattering intensities at lower q values (Figure 3) can be associated with size variations and interactions between the large compound particles. In the intermediate window of scattering wavevectors, however, the power law description conveys no physical meaning. The values in Table 2 are given to complete the information and for the sake of comparison. However, the increase of the scattering at the intermediate q range with increasing temperature can be attributed to formation of domains, presumably composed of PPO. It is noteworthy that at the highest q range all curves overlap and exhibit slopes closed to 2 (Table 2), which indicates the presence of thin Gaussian chains that are practically not affected by the variations in temperature. Briefly, it seems that coexistence of PPO domains and Gaussian chains is observed. On the q scale of SANS measurements they may be regarded as individual entities inside the large compound particles.

The effects of temperature and copolymer composition are presented in Figure 4. It should be noted that the difference in the scattering contrasts of the PPO and PG moieties (-5.96×10^{10} and -5.40×10^{10} cm^{-2}, respectively) is very small and can be considered negligible. At 15 °C (Figure 4a) the scattering from the solutions of LGP63, LGP67, and LGP68 at intermediate and high q ranges is similar, and the scattering profiles fall into a common master curve. The scattering from LGP68+ is lower at intermediate q range and comparable to that of the rest of the copolymers at the highest q. Again the slopes at the highest q range are ca. 2 (Table 2), which, as indicated above, is consistent with the presence of Gaussian chains. In line with the expectations, no scattering that could be associated with the presence of PPO domains was observed. Indeed, as shown elsewhere,[30] the lower critical solution temperature (LCST) of PPO of molecular weight of 2000 in water is 19 °C. LCST of several degrees lower is to be expected in D_2O, which indicates that at 15 °C PPO is below but close to the LCST. At the lowest q range, however, again traces of scattering from very large particles are observed. We have shown previously[23] that the solubility of PG changes in a completely opposite fashion to that of PPO, that is, decreases with decreasing temperature. Therefore, this scattering could be related with the presence of large loose particles resulting from the lowered solubility of PG and the approximity of PPO to its LCST.

The increase of temperature to 40 and 60 °C, which are well above the LCST of PPO, brings about to significant changes in the scattering profiles (Figure 4b,c). At intermediate q scattering from compact domains is observed. The most noticeable are the changes of the scattering profile of LGP63 showing a maximum at intermediate q range and a substantial decrease of the slope at lower q (Figure 4b). At 60 °C the curve of LGP63 is somewhat shifted toward lower scattering with no clear maximum (Figure 4c), most probably indicating phase separation. This observation is additionally supported by the incoherent scattering at lower q. This scattering is directly connected with the concentration of H in solution, and obviously it is much lower at 60 °C. The peculiar scattering curve at 40 °C is in line with this finding. At this temperature the system is seemingly close to phase separation, and the further increase in temperature leads to dramatical growth of the PPO domains.

The scattering profiles of the rest of the copolymers studied keep changing with increasing temperature in that, for example, the slightly pronounced shoulder-like patterns at $q = (3-5) \times 10^{-2}$ Å^{-1} tend to convert into more pronounced ones as the temperature increases from 40 to 60 °C (Figure 4b,c). Although different, the common feature of the scattering curves is that the intensities of the "shoulders" in the above q range were found to decrease with increasing PG content.

The whole q range was analyzed using an indirect Fourier transformation (IFT) approach developed by Glatter[31] in the version of Pedersen et al.[32] The following assumptions were made: (i) the trace scattering from large particles was approximated by the power law $q^{-\alpha}$, and (ii) the studied domains were spherical 3D objects. The best fits were obtained when $\alpha = 2.8$, which, in very good agreement with the light scattering data,[24] can be connected with noncompact structure of large aggregates. According to Schmidt,[33] a value of α in the range between 1 and 3 points on mass fractal structure with relation between mass of aggregate M and linear size l as $M \sim l^{Dm}$ where Dm is fractal dimension and $Dm = \alpha$. An additional analysis was made in the q interval from 0.02 to 0.3 Å^{-1}; that is, the lowest q interval was excluded and the term of trace scattering from large particles was not presented. The two analyses gave the same parameters, which indicated that the contribution of the trace scattering from large aggregates and that from the 3D domains do not interfere. The parameter obtained from IFT is

Table 2. Slopes Determined as $I(q) \sim q^{-\alpha}$ at Different q Ranges for the Low Concentrated Solutions of the Copolymers Studied

system	0.005−0.009	0.009−0.03	0.05−0.1	0.1−0.3
LGP63, 2.15 wt %				
15 °C	1.92 ± 0.01	2.90 ± 0.03	0.757 ± 0.001	1.84 ± 0.04
40 °C				1.89 ± 0.05
60 °C				
LGP67, 2.12 wt %				
15 °C	2.67 ± 0.01	2.82 ± 0.02	0.87 ± 0.01	1.81 ± 0.04
40 °C	1.71 ± 0.01	1.17 ± 0.02	4.03 ± 0.08	1.87 ± 0.04
60 °C	1.41 ± 0.03	0.73 ± 0.02	4.8 ± 0.2	1.99 ± 0.04
LGP68, 2.15 wt %				
15 °C	2.36 ± 0.06	3.13 ± 0.02	0.91 ± 0.02	1.90 ± 0.04
40 °C	1.83 ± 0.06	1.75 ± 0.02	3.9 ± 0.1	1.93 ± 0.03
60 °C	1.52 ± 0.03	1.08 ± 0.02	4.7 ± 0.1	1.97 ± 0.03
LGP68+, 2.15 wt %				
15 °C	4.04 ± 0.04	2.45 ± 0.05	0.92 ± 0.01	1.68 ± 0.04
40 °C	1.82 ± 0.01	1.19 ± 0.02	2.37 ± 0.01	1.72 ± 0.03
60 °C	~ 0.5	0.44 ± 0.04	4.04 ± 0.07	1.75 ± 0.04

Table 3. Cross-Sectional Scattering at Zero Angle ($I(0)$), Cross-Sectional Radius of Gyration (R_g), Volume (V), and Aggregation Number (N_{agg}) of the PPO Domains and Number of PPO Domains ($N_{domains}$) per Large Compound Particles Formed in Aqueous Solution by the Copolymers Studied

	$I(0)$	R_g (Å)	V (Å^3)	N_{agg}	$N_{domains}$
LGP63, 2.15 wt %					
40 °C	80 ± 4	103 ± 4			
60 °C	3.77 ± 0.03	47 ± 2			
LGP67, 2.12 wt %					
15 °C	0.055 ± 0.003	12.1 ± 0.5	2 108		
40 °C	4.07 ± 0.07	38.2 ± 0.3	155 971	48	69
60 °C	7.9 ± 0.2	39.0 ± 0.4	302 745	92	10
LGP68, 2.15 wt %					
15 °C	0.047 ± 0.002	11.5 ± 0.5	2 704		
40 °C	2.77 ± 0.06	42.0 ± 0.4	159 338	49	19
60 °C	6.2 ± 0.1	40.9 ± 0.4	356 641	109	3
LGP68+, 2.15 wt %					
15 °C	0.091 ± 0.002	15.4 ± 0.2	6 543		
40 °C	1.85 ± 0.03	47.2 ± 0.4	133 021	41	24
60 °C	4.74 ± 0.07	39.3 ± 0.3	340 822	104	

the cross-sectional pair distance distribution function, $p(r)$. The functions for the solution of LGP67 at 40 and 60 °C are plotted in Figure 5. The shape of the two functions is quite symmetrical, implying that the domains are close to spherical. The scattering at zero angle, $I(0)$, and cross-sectional radius of gyration, R_g, were determined from the pair distribution functions. The values of the two quantities are collected in Table 3.

R_g is related to the size of the domains and distribution of scattering length density within domains (eq 1).

$$R_g = \left[\frac{\int_0^D r^2 p(r)\,dr}{\int_0^D p(r)\,dr}\right]^{1/2} \quad (1)$$

As seen from Table 3, the values of R_g at 15 °C are considerably lower than those at elevated temperatures, which can be easily rationalized as a consequence of the solvent quality increase for PPO with decreasing temperature. Obviously, at 15 °C small size domains, predomains, exist. Possibly they serve as nucleation centers for formation at elevated temperatures of the PPO domains. Considering the lowered solubility of the PG moieties at lower temperatures,[23] the composition of the predomains might be rather different from that of the domains at elevated temperatures with considerable contribution of PG.

The increase in temperature from 40 to 60 °C does not affect the size of the domains (exception LGP68+) but gives rise to an increase in $I(0)$ (Table 3), which indicates increasing volume fraction of the PPO domains. In other words, upon a temperature increase more PPO domains are formed.

The value of R_g for LGP68+ at 40 °C is somewhat erratic. The larger R_g could be attributed to shape transitions of the domains evidenced by asymmetricity of the pair distance distribution function (not shown). Another study aiming to detect possible shape transitions is in progress and the results will be reported separately.

The equivalent sphere radius, r, can be calculated from R_g as (eq 2).

$$r = (5/3)^{1/2} R_g \quad (2)$$

It is typically about 50 Å, which is slightly below $D_{max}/2$ with D_{max} being a maximal diameter input in the IFT model. This finding implies that the domains are slightly prolate objects.

The data at $q > 0.1$ Å^{-1} were analyzed to estimate the dimensions of the unassociated copolymer chains in the large particles. Regardless of the temperature and copolymer composition the average cross-sectional diameter of these structures was estimated to ca. 10−20 Å, which is fairly consistent with the size of the individual copolymer chains. These chains are not involved in the formation of the PPO domains; however, the chains mediate the interdomain interactions as shown in Figure 6. Upon a temperature increase fractions of the individual chains driven by the enhancing hydrophobicity of the PPO moieties start to self-associate into domains, thus bringing about to the overall increase in the volume of the latter.

The aggregation number (N_{agg}) of the PPO domains, that is, the number of the PPO chains per domain, can be estimated from the volume of the domain (V) and the PPO volume (V_{PPO}) under the assumptions that the domains are built by PPO and all PPO is in the domains. Here, V is calculated using eq 3

$$I(0) = \phi \Delta\rho^2 V \quad (3)$$

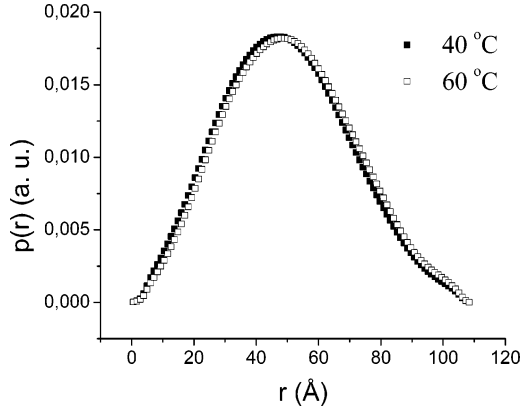

Figure 5. Pair distance distribution functions obtained from the SANS data of 2.12 wt % solution of LGP67 in D_2O at 40 and 60 °C.

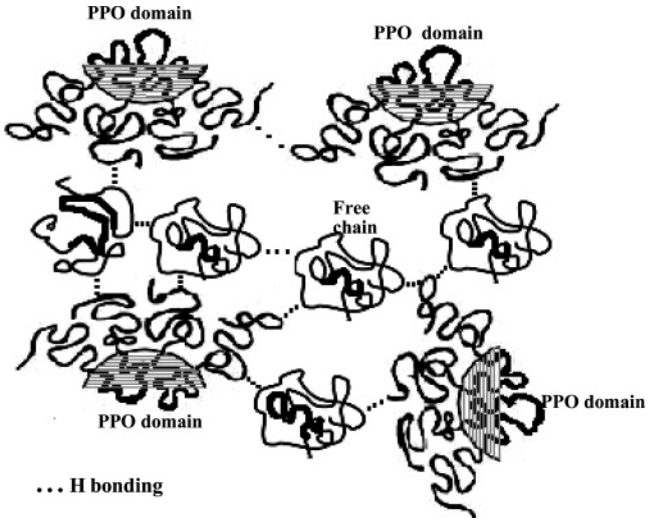

Figure 6. Schematic representation of a part of the interior of a large compound particle formed by the LGP copolymers in aqueous solution. The wide curved lines represent PG chains, which are interconnected with other PG chains by hydrogen bonding (short dotted lines). The thick curved lines represent PPO chains.

with ϕ being the PPO volume fraction and $\Delta\rho$ the difference between the scattering length densities of PPO (0.343×10^{10} cm^{-2} [12a]) and D_2O (6.33×10^{10} cm^{-2}), whereas V_{PPO} is given by the product $34V_{PO}$, where V_{PO} (= 96.3 $Å^3$) and 34 are the volume of the propylene oxide monomer unit[12a] and the degree of polymerization of the PPO block, respectively. The resulting values are presented in Table 3.

The above assumptions, however, are not fulfilled. As repeatedly shown, scattering from Gaussian chains was observed in the investigated temperature and concentration ranges and coexistence of PPO domains and unassociated chains inside the large compound particles was suggested. Strong arguments are also the increase of V with increasing temperature (Table 3) and the fact that the volume fraction of the PPO domains calculated from R_g was invariably lower (by a factor of 3.3−7.2 and 1.6−1.8 at 40 and 60 °C, respectively) than the PPO volume fraction taken from the overall stoichiometry. Consequently, we may assume that N_{agg} in Table 3 is overestimated by a similar factor. Last but not least, by combining the light scattering and SANS data, we tried to estimate the number of PPO domains per large compound particle ($N_{domains}$). $N_{domains}$ was estimated by dividing the aggregation number of the large compound particles determined by static light scattering[24] by the corrected aggregation number of the domains. The resulting values are included in Table 3. The dramatic change of $N_{domains}$ upon increasing temperature from 40 to 60 °C reflects the changes of the solvent quality. It changes in opposite fashions for PPO and PG: whereas for the former the solvent quality worsens, which leads to an increase in N_{agg} (Table 3), for the latter it gradually improves[23] and leads to a decrease in the aggregation number of the large compound particles.[24] As a result of the superposition of the two opposite processes, dramatic changes in $N_{domains}$ were observed (Table 3).

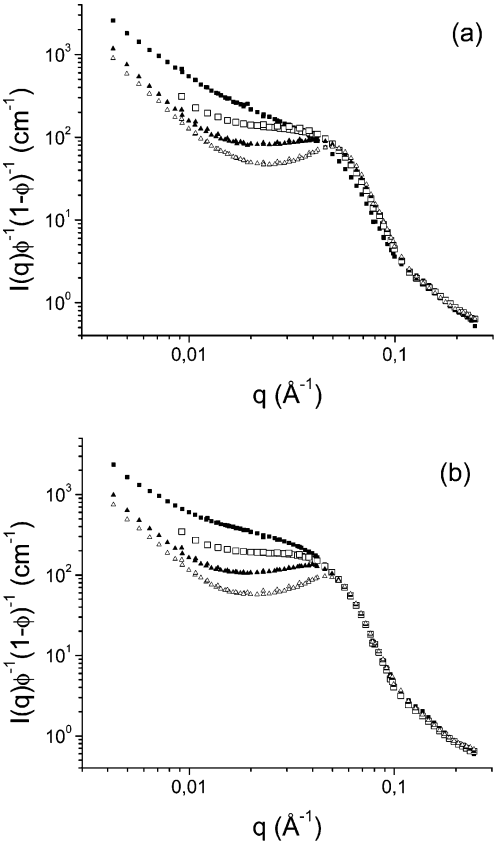

Figure 7. SANS data of LGP67 solutions measured at 40 (a) and 60 °C (b) and concentrations of 2% (filled squares), 10% (empty squares), 20% (filled triangles), and 33% (empty triangles). Scattering intensities are normalized to $\phi(1 - \phi)$, where ϕ is the copolymer volume fraction.

High Concentrated Solutions. Measurements as a function of temperature, concentration, and copolymer composition were performed in the 10−33 wt % range. For the sake of clarity the scattering data were normalized to $\phi(1 - \phi)$, where ϕ is the volume fraction. In such a way of presentation the scattering intensity should depend only on the size and interactions of scattering objects and should perfectly overlap if these parameters are not affected by concentration. The normalization to $\phi(1 - \phi)$ has been frequently applied to two-phase and multiphase systems.[34] It provides more consistent results in a wide q range, especially for concentrated samples in contrast to the normalization to ϕ; the latter typically gives a significant decrease of the normalized scattering intensity. This can be interpreted as a decrease of the domain size with increasing concentration, which is not realistic.

Figure 7 shows the scattering profiles of LGP67 at 40 and 60 °C and different concentrations. The rest of the copolymers studied exhibit similar scattering profiles. LGP63 at concentrations 10 and 20 wt % was found to phase separate. The scattering curves fully overlap in the q range 0.1−0.3 $Å^{-1}$ which, as discussed above, corresponds to scattering from flexible Gaussian chains. At the lowest q scattering intensities

significantly decrease with increasing concentration, which can be related to interactions between the large aggregates. At intermediate q maxima appeared. As the concentration increased they became more pronounced, which revealed significant interactions between the neighboring domains, and were found to shift to larger q (Figure 7). Beyond the correlation peaks, that is, in the q range 0.06−0.1, the scattering curves at 40 °C (Figure 7a) do not overlap; instead, the scattering increases with increasing concentration. This indicates the absence of distinct interfaces between the domains and the continuous interior of the large compound particles. Obviously, at 40 °C the formation of the domains has not been completed yet; they are flexible and do not have a sharp interface. The situation is different at 60 °C (Figure 7b): the scattering curves completely overlap at intermediate and high q (0.06−0.3 Å), that is, in the length scale of Gaussian chains and domain interface. We can suggest that at this temperature the domain formation is completed, and the further increase in concentration leads to increasing number of domains. The position of q_{max} shifts to larger q values approximately as $q_{max} \sim c^{1/3}$, which is consistent with an arrangement of the domains in cubic symmetry.[35] Interestingly, reasonable agreement between the uncorrected N_{agg} (Table 3) and N_{agg} values calculated via eq 4, assuming a simple cubic arrangement was found. Future experiments are planned to identify the phases.

$$N_{agg} = a^{-1} c N_A (2\pi/q_{max})^3 \quad (4)$$

Here, N_A is the Avogadro number, c is the concentration of PPO, and $a = 1$, $2^{-1/2}$, or $4/3^{3/2}$ for simple cubic, body-centered cubic, and face-centered cubic phases, respectively.

Conclusions

The internal structure of large compound particles formed by a series of block copolymers based on PPO and PG in aqueous solution was investigated by SANS. The results indicate coexistence of slightly prolate spherical PPO domains and individual Gaussian chains that mediate the interactions between the domains in the interior of the large particles. Structural parameters based on fits to compact spheres and flexible chains and on the IFT method are given. The number of the PPO chains in one domain was determined at different temperatures as well. By combining earlier light scattering data[24] and the results from the present study the number of the PPO domains, $N_{domains}$, per compound particle was estimated. The dramatic decrease in $N_{domains}$ was attributed to superposition of two opposite processes, resulting in simultaneous (i) decrease of the aggregation number of the large particles[24] and (ii) increase of the number of PPO chains in the domains. At higher concentrations the PPO domains are supposedly arranged in a cubic lattice as judged from the scaling of q_{max} with $c^{1/3}$.

Acknowledgment. The project was supported by the European Commission under the 6th Framework Programme through the Key Action: Strengthening the European Research Area, Research Infrastructures (Contract RII3-CT-2003-505925). Thanks are due to Professor Mats Almgren, University of Uppsala, for critically reading the manuscript and worthwhile discussions.

References and Notes

(1) Mortensen, K.; Pedersen, J. S. *Macromolecules* **1993**, *26*, 805−12.
(2) Glatter, O.; Scherf, G.; Schillen, K.; Brown, W. *Macromolecules* **1994**, *27*, 6046−54.
(3) King, S. M.; Heenan, R. K.; Cloke, V. M.; Washington, C. *Macromolecules* **1997**, *30*, 6215−22.
(4) Schillen, K.; Brown, W.; Johnsen, R. *Macromolecules* **1994**, *27*, 4825−32.
(5) Jorgensen, E. B.; Hvidt, S.; Brown, W.; Schillen, K. *Macromolecules* **1997**, *30*, 2355−64.
(6) Al-saden, A. A.; Whately, T. L.; Florence, A. T. *J. Colloid Interface Sci.* **1982**, *90*, 303−9.
(7) Almgren, M.; Brown, W.; Hvidt, S. *Colloid Polym. Sci.* **1995**, *273*, 2−15.
(8) Mortensen, K.; Brown, W. *Macromolecules* **1993**, *26*, 4128−35.
(9) Brown, W.; Schillen, K.; Hvidt, S. *J. Phys. Chem.* **1992**, *96*, 6038−44.
(10) Bahadur, P.; Pandya, K. *Langmuir* **1992**, *8*, 2666−70.
(11) Mortensen, K.; Brown, W.; Norden, B. *Phys. Rev. Lett.* **1992**, *68*, 2340−3.
(12) (a) Mortensen, K. *Colloids Surf., A* **2001**, *183*, 277−92. (b) Hamley, I. W. *Curr. Opin. Colloid Interface Sci.* **2000**, *5*, 342−50. (c) Eiser, E.; Molino, F.; Porte, G.; Pithon, X. *Rheol. Acta* **2000**, *39*, 201−8. (d) Mortensen, K. *Macromolecules* **1997**, *30*, 503−7.
(13) Linse, P. *Macromolecules* **1993**, *26*, 4437−49.
(14) (a) Mortensen, K.; Brown, W.; Jorgensen, E. *Macromolecules* **1995**, *28*, 1458−63. (b) Mortensen, K. *Polym. Adv. Technol.* **2001**, *12*, 2−22. (c) Svenson, B.; Olsson, U.; Alexandridis, P. *Langmuir* **2000**, *16*, 6839−46.
(15) (a) Caragheorgheopol, A.; Pilar, J.; Schlick, S. *Macromolecules* **1997**, *30*, 2923−33. (b) Senkow, S.; Mehta, S. K.; Douheret, G.; Roux, A. H.; Roux-Desgranges, G. *Phys. Chem. Chem. Phys.* **2002**, *4*, 4472−80. (c) Alexandridis, P.; Olsson, U.; Lindman, B. *Langmuir* **1998**, *14*, 2627−38. (d) Alexandridis, P.; Zhou, D.; Khan, A. *Langmuir* **1996**, *12*, 2690−700.
(16) Wanka, G.; Hoffmann, H.; Ulbricht, W. *Macromolecules* **1994**, *27*, 4145.
(17) Almdal, K.; Bates, F. S.; Mortensen, K. *J. Chem. Phys.* **1992**, *96*, 9122.
(18) Yang, L.; Badells, A. D.; Attwood, D.; Booth, C. *J. Chem. Soc., Faraday Trans.* . **1992**, *88*, 1447−52.
(19) (a) Nace, V. M. *J. Am. Oil Chem. Soc.* **1996**, *73*, 1. (b) Altinok, H.; Yu, G.-E.; Nixon, S. K.; Gorry, P. A.; Attwood, D.; Booth, C. *Langmuir* **1997**, *13*, 5837−48. (c) Altinok, K.; Nixon, S. K.; Gorry, P. A.; Attwood, D.; Booth, C.; Kelarakis, A.; Havredaki, V. *Colloids Surf., B* **1999**, *16*, 73−91. (d) Booth, C.; Yu, G.-E.; Nace, V. M. in *Amphiphilic Block Copolymers Self-Assembly and Applications*; Alexandridis, P., Lindman, B., Eds.; Elsevier Science: Amsterdam, 2000; Chapter 4.
(20) Booth, C.; Attwood, D. *Macromol. Rapid Commun.* **2000**, *21*, 501−27.
(21) (a) Bedells, A. D.; Arafeh, R. M.; Yang, Z.; Attwood, D.; Heatley, F.; Padget, J. C.; Price, C.; Booth, C. *J. Chem. Soc., Faraday Trans.* **1993**, *89*, 1235−42. (b) Yang, Z.; Pickard, S.; Deng, N.-J.; Barlow, R. J.; Attwood, D.; Booth, C. *Macromolecules* **1994**, *27*, 2371−9. (c) Zhou, Z.; Chu, B.; Nace, V. M. *Langmuir* **1996**, *12*, 5016−21. (d) Zhou, Z.; Chu, B.; Nace, V. M.; Yang, Y.-W.; Booth, C. *Macromolecules* **1996**, *29*, 3663−4. (e) Liu, T.; Nace, V. M.; Chu, B. *J. Phys. Chem. B* **1997**, *101*, 8074−8. (f) Chaibundit, C.; Mai, S.-M.; Heatley, F.; Booth, C. *Langmuir* **2000**, *16*, 9645−52.
(22) (a) Deng, Y.; Ding, J.; Stubbersfield, R. B.; Heatley, F.; Price, C.; Booth, C. *Polymer* **1992**, *33*, 1963. (b) Ding, J.; Attwood, D.; Price, C.; Booth, C. *Eur. Polym. J.* **1991**, *27*, 901. (c) Yang, Z.; Yang, Y.-W.; Zhou, Z.-K.; Attwood, D.; Booth, C. *J. Chem. Soc., Faraday Trans.* **1996**, *92*, 257−65. (d) Schillen, K.; Claesson, P. M.; Malmsten, M.; Linse, P.; Booth, C. *J. Phys. Chem. B* **1997**, *101*, 4238−52.
(23) Halacheva, S.; Rangelov, S.; Tsvetanov, Ch. *Macromolecules* **2006**, *39*, 6845−52.
(24) Rangelov, S.; Almgren, M.; Halacheva, S.; Tsvetanov, Ch. *J. Phys. Chem. C* **2007**, *111*, 13185−91.
(25) (a) Hasagawa, H.; Hashimoto, T.; Kawai, H.; Lodge, T.; Amis, E.; Glinka, C.; Han, C. *Macromolecules* **1985**, *18*, 67−78.
(26) (a) Mortensen, K. *Curr. Opin. Colloid Interface Sci.* **1998**, *3*, 12. (b) Pedersen, J. S.; Svaneborg, C. *Curr. Opin. Colloid Interface Sci.* **2002**, *7*, 158. (c) Castalletto, V.; Hamley, I. W. *Curr. Opin. Colloid Interface Sci.* **2002**, *7*, 167.
(27) (a) Zipfel, J.; Lindner, P.; Tsianou, M.; Alexandridis, P.; Richtering, W. *Langmuir* **1999**, *15*, 2599−602. (b) Pospisil, H.; Plestil, J.; Tuzar, Z. *Collect. Czech. Chem. Commun.* **1993**, *58*, 2428−35. (c) Hecht, E.; Mortensen, K.; Hoffmann, H. *Macromolecules* **1995**, *28*, 5465−76. (d) Mortensen, K. *Phys. Rev. Lett.* **1993**, *71*, 1728−31. (e) Habas, J.-P.; Pavie, E.; Lapp, A.; Peyrelasse, J. *J. Rheol.* **2004**, *48*, 1−21.
(28) Stuhrmann, H. B.; Burkhardt, N.; Dietrich, G.; Junemann, R.; Meerwinck, W.; Scmitt, M.; Wadzak, J.; Willumeit, R.; Zhao, J.; Nierhaus, K. H. *Nucl. Instrum. Methods* **1995**, *A356*, 133.
(29) Pedersen, J. S.; Posselt, D.; Mortensen, K. *J. Appl. Crystallogr.* **1990**, *23*, 321.

(30) (a) Malmsten, M.; Linse, P.; Zhang, K.-W. *Macromolecules* **1993**, *26*, 2905. (b) Mortensen, K.; Schwahn, D.; Janssen, S. *Phys. Rev. Lett.* **1993**, *71*, 1728. (c) Schild, H. G.; Tirell, D. A. *J. Phys. Chem.* **1990**, *94*, 4352.
(31) Glatter, O. *J. Appl. Crystallogr.* **1977**, *10*, 415−421.
(32) Hansen, S.; Pedersen, J. S. *J. Appl. Crystallogr.* **1991**, *24*, 541−548.
(33) Schmidt, P. W. In *Modern Aspects of Small-Angle Scattering*; Brumberger, H., Ed.; Kluwer Academic Publishers: Dordrecht, The Netherlands, 1995; pp 1−56.
(34) Feigin, L. A.; Svergun, D. I. In *Structure Analysis by Small-Angle X-ray and Neutron Scattering*; Taylor, G. W., Ed.; Plenum: New York, 1987.
(35) (a) Boden, N. In *Micelles, Membranes, Microemulsions and Monolayers*; Gelbert, W. M., Ben-Shaul, A., Roux, D., Eds.; Springer-Verlag: New York, 1994. (b) Chen, S. H.; Sheu, E. Y.; Kalus, J.; Hoffmann, H. *J. Appl. Crystallogr.* **1988**, *21*, 751.

MA071151Q